# Nonlinear time history analysis of large concrete dam considering near-field earthquake effect

Ravi Sharma Bhandari[1], Hari Ram Parajuli[2]

[1] *Department of Civil Engineering, IOE, Central Campus, Pulchowk, Tribhuvan University, Nepal*

[2] *Department of Civil Engineering, IOE, Thapathali Campus, Thapathali, Tribhuvan University, Nepal*

Corresponding Email: rsbhandari@outlook.com

**Abstract:** Concrete gravity dam (140 m high) of proposed Tanahu Hydroelectric project (140 MW), Nepal has been modelled in SAP2000 for this study. The entire modelling is based on US-Army Engineering Manuals. Near-field earthquake effect is studied and compared with the far field counterpart. Linear and Nonlinear time-history analysis are used to assess earthquake performance of non-overflow gravity dam section. The results of linear time history analysis are compared with the EM 1110-2-6051 and EM 1110-2-6053 performance acceptance criteria for gravity dams. This study indicated that the dam would suffer significant cracking along the base for all the fifteen selected near-field earthquake record and should be assessed on the basis of nonlinear time-history analysis. This study also concluded that near-field earthquake with higher PGV may affect more than that having more PGA but lower PGV. At the other hand, response for far-field earthquake response indicates that the dam will not suffer profoundly. This concludes that, while performing the analysis of large dams in tectonically active country like Nepal, it would be more appropriate to use the near-field records than code based method or far-field earthquake records.

**Keywords:** Gravity dam, near-field, earthquake, linear time history, nonlinear time history

## 1. Introduction

Nepal has large potential of hydropower resources, however it is located in one of the most tectonically active regions of the world. Government of Nepal is planning several large hydro-powers to meet increasing demand of electricity which requires large concrete dams. The risk of failure of dam cannot be ignored due to high seismic activity.

Two important instances of earthquakes damage to concrete dams occurred in the 1960s: Hsinfengkiang in China and Koyna in India. The damage was severe enough in each case to need major repairs and strengthening, however the reservoirs weren't released, thus there was no flooding damage. This wonderful safety record, however, is not sufficient reason for satisfaction regarding the seismic safety of concrete dams, as a result of no such dam has yet been subjected to must conceivable earthquake shaking. For this reason it's essential that every existing concrete dams in tectonically active regions, also as new dams planned for such regions, be checked to see that they're going to perform satisfactorily throughout the great earthquake shaking to which they might be subjected especially in the near -field regions.

## 2. Near-Fault Earthquake Record Characteristics

The near-field ground motions are characterized by high peak acceleration (PGA), high peak velocity (PGV), high peak displacement (PGD), pulse-like time history and distinct spectral content. Criteria for Near-Field earthquake record (Table 1) are evaluated based on the paper "Identification of Near-Fault Earthquake record Characteristics" [1].

**Table 1: Ground motion parameters, measured characteristics and lower-bound values**

| Ground Motion parameters | Ground Motion Characteristics | | | | |
|---|---|---|---|---|---|
| | Amplitude | Frequency Content | Duration | Energy | Lower-Bound |
| PGA | √ | | | √ | 0.2 g |
| CAV | √ | | | √ | 0.30 g sec |
| PGV | √ | | | √ | 20 cm/s |
| $I_A$ | √ | | √ | | 0.4 m/sec |
| I | √ | | √ | | 30 cm sec$^{-0.75}$ |
| $a_{rms}$ | √ | √ | √ | | 0.5 m/sec$^2$ |

This procedure has been applied in the selected ground motion data from PEER ground motion database [2] to recognize near-field records.

Seven near-fault earthquake events recorded at fifteen different recording stations (Table 2) and five far-fault earthquakes recorded at different five recording stations (Table 3), respectively, are selected for the evaluation of response of gravity dam. Selected ground motion records are evaluated according to above characteristics. Typical near-field fault normal

components of acceleration and velocity time histories are shown in Figure 1 and Figure 2, respectively.

**Table 2: Selected near-fault ground motion records**

| SN | NGA# | Event | Year | Mag. | Epc. Dist. (km) |
|----|------|-------|------|------|-----------------|
| 1 | 181 | Imperial Valley-06 | 1979 | 6.53 | 0 |
| 2 | 182 | Imperial Valley-06 | 1979 | 6.53 | 0.6 |
| 3 | 779 | Loma Prieta | 1989 | 6.93 | 0 |
| 4 | 821 | Erzican- Turkey | 1992 | 6.69 | 0 |
| 5 | 825 | Cape Mendocino | 1992 | 7.01 | 0 |
| 6 | 828 | Cape Mendocino | 1992 | 7.01 | 0 |
| 7 | 879 | Landers | 1992 | 7.28 | 2.2 |
| 8 | 1044 | Northridge-01 | 1994 | 6.69 | 3.2 |
| 9 | 1063 | Northridge-01 | 1994 | 6.69 | 0 |
| 10 | 1084 | Northridge-01 | 1994 | 6.69 | 0 |
| 11 | 1085 | Northridge-01 | 1994 | 6.69 | 0 |
| 12 | 1086 | Northridge-01 | 1994 | 6.69 | 1.7 |
| 13 | 1106 | Kobe- Japan | 1995 | 6.9 | 0.9 |
| 14 | 1119 | Kobe- Japan | 1995 | 6.9 | 0 |
| 15 | 1120 | Kobe- Japan | 1995 | 6.9 | 1.5 |

**Table 3: Selected far-fault ground motion records**

| SN | NGA# | Event | Year | Mag. | Epc. Dist. (km) |
|----|------|-------|------|------|-----------------|
| 1 | 166 | Imperial Valley-06 | 1979 | 6.53 | 50 |
| 2 | 826 | Cape Mendocino | 1992 | 7.01 | 42 |
| 3 | 832 | Landers | 1992 | 7.28 | 69 |
| 4 | 948 | Northridge-01 | 1994 | 6.69 | 41 |
| 5 | 1105 | Kobe- Japan | 1995 | 6.9 | 95 |
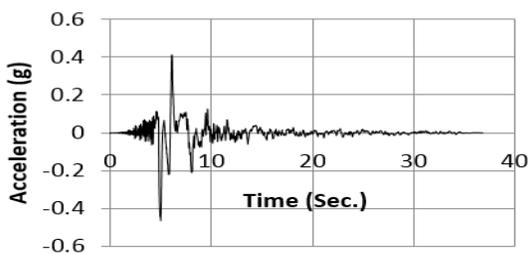


**Figure 1: Near-field Fault Normal acceleration time history (Imperial Valley – 06 (Recording station: El Centro Array#7)**
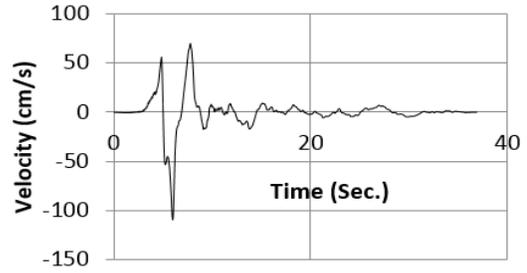


**Figure 2: Near-field Fault Normal velocity time history (Imperial Valley – 06 (Recording station: El Centro Array#7)**

## 3. Finite Element Modeling of Gravity Dam and Material Properties

The dam and foundation rock are represented by 2D plane strain elements of unit thickness with concrete and rock properties, respectively. A modulus of elasticity of 22360 N/mm$^2$, a Poisson's ratio of 0.19, with a unit weight of 2500 kg/m$^3$ is assumed for mass concrete. The foundation rock is assumed massless and its modulus and Poisson's ratio were assumed to be represented by 38000 N/mm$^2$ [3] and 0.151. The inertia forces of the impounded water were represented by added hydrodynamic mass values in accordance with the generalized Westergaard method. The added mass associated with nodal points on the sloped portion of the upstream face consists of horizontal and vertical values. Thus they generate inertia forces in the horizontal and vertical direction. The finite element model is shown in Figure 3. A total of 17400 plane strain element were used: 9900 elements to model the dam and 7500 to model the foundation rock. The model includes a total number of 17799 nodal points. Length of the foundation model is 450 m and depth is 150 m which satisfy the criteria specified in *EM 1110-2-6051* [4]. Equation of motion for the complete system is

$$(m_s + m_a)\ddot{r} + c\dot{r} + kr = -(m_s + m_a)l_x a_{gx}(t)$$

$$-(m_s + m_a)l_y a_{gy}(t) - (m_s + m_a)l_z a_{gz}(t) \quad \ldots\ldots (1)$$

Where

$m_s$ = mass matrix of the structure

$m_a$ = added hydrodynamic mass matrix having non-zero terms only at the structure-water nodal points

$\dot{r}, \ddot{r}$ = velocity and acceleration vectors, respectively

---

[1] Properties of Rock Materials

*Nonlinear time history analysis of large concrete dam considering near-field earthquake effect*

$c$ = overall damping matrix for the entire system

$k$ = Combined stiffness matrix for structure and foundation region

$r$ = vector of nodal point displacements for the complete system relative to the rigid base displacement

$l_x, l_y, l_z$ = Direction cosines to x, y and z-DOF's respectively

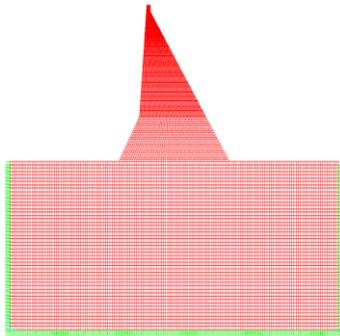$a_{gx}(t), a_{gy}(t), a_{gz}(t)$ = Ground acceleration input in x-, y-, and z-direction respectively

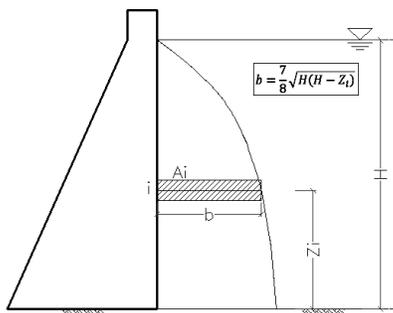

**Figure 3: Dam-foundation model in SAP2000**



**Figure 4: Westergaard added-mass representation**

**(Source: EM-1110-2-6051)**

The fluid structure interaction (Figure 4) has been modelled according to the Westergaard (1933).

$$m_{ai} = \frac{7}{8} \rho_w \sqrt{H(H - z_i)} \, A_i \qquad \text{.........(2)}$$

Where

      H = depth of water

      $z_i$ = height above the base of the dam

      $A_i$ = tributary surface area at point i

## 4. Structural Performance and Damage Criteria

Structural performance and damage criteria is checked according to the US Army Engineering manual [4]. The dam is first checked for linear response by linear time history analysis and if the linear response crosses the acceptable limit (Figure 5) then nonlinear time history analysis has been performed. The different load combinations for static and dynamic stresses for 2D analysis according to EM-1110-2-6053 [5] has been shown in Table 4.
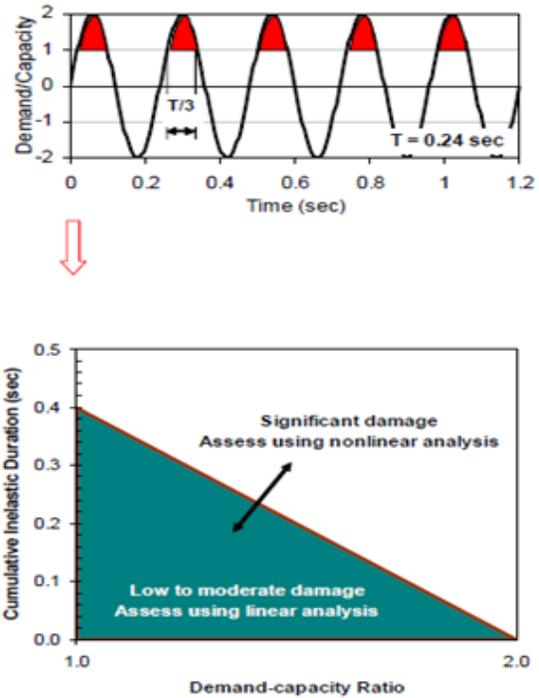




**Figure 5: Basis for upper limit demand-capacity ratio and cumulative inelastic duration**

**(Source: EM-1110-2-6051)**

**Table 4: Load combination cases for combining static and dynamic stresses for 2D analysis**

| Case | Seismic Loads | | Static Loads (Stress) |
|---|---|---|---|
| | Vertical (V) | Horizontal (H) | |
| Case 1 (Static + H + V) | + | + | + |
| Case 2 (Static - H + V) | + | - | + |
| Case 3 (Static + H - V) | - | + | + |
| Case 4 (Static - H - V) | - | - | + |

## 5. Linear Time History Analysis

Before nonlinear analysis linear response of the dam is performed. If linear response is within the performance

limit nonlinear analysis is not necessary. Equation of motion [6] for linear analysis may be expressed as

$$m\ddot{u}(t) + c\dot{u}(t) + ku(t) = p(t) \qquad .........(3)$$

Where m, c, and k are the mass, damping and stiffness, respectively. $u(t), \dot{u}(t) \ and \ \ddot{u}(t)$ are respectively nodal displacement, velocity and acceleration vectors and $p(t)$ is the effective load vector.

The mode shapes corresponding to the first five natural periods are shown in Table 5.

**Table 5: Natural frequencies for first five mode shapes**

| Mode | Period, Seconds | Frequency, Hz |
|------|----------------|---------------|
| 1 | 0.47 | 2.12 |
| 2 | 0.23 | 4.35 |
| 3 | 0.19 | 5.26 |
| 4 | 0.13 | 7.69 |
| 5 | .09 | 11.11 |

Linear response of the proposed dam is evaluated which shows large stress at the upstream face where the profile changes the slope (Figure 6). To overcome this issue the upstream profile has been modified which reduces the high stress concentration at that point. Result for modified section with a flat curve at upstream face greatly reduces the stress concentration problem (Figure 7). The stress is distributed to the large area due to the smooth transition.
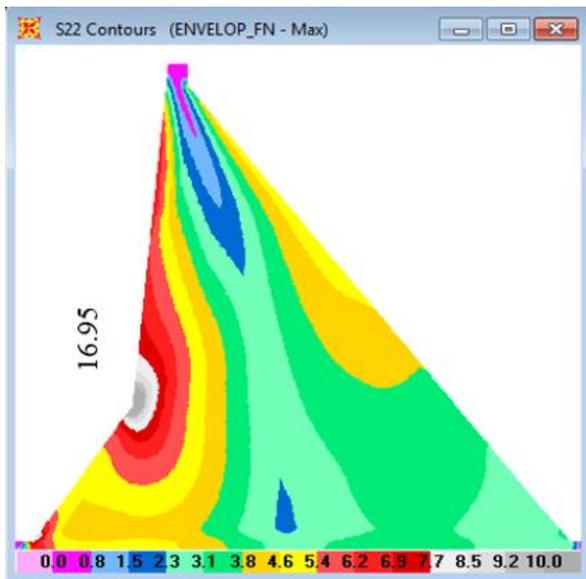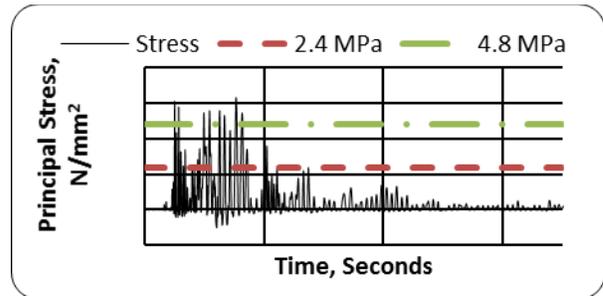


**Figure 6: Envelope of maximum vertical stresses (N/mm²) for proposed section.**
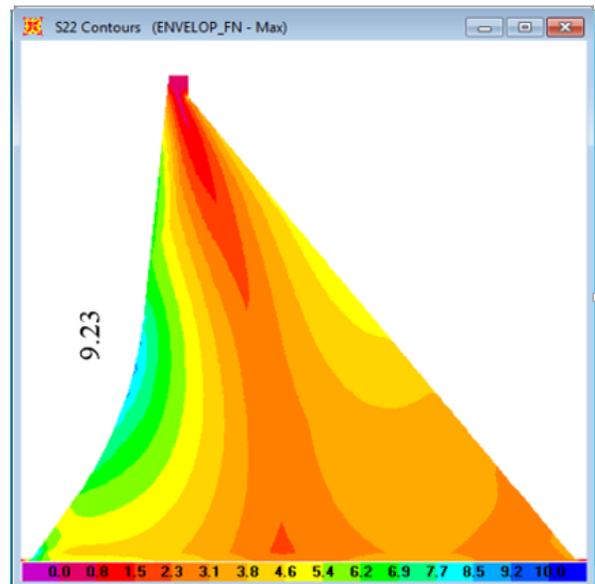


**Figure 7: Envelope of maximum vertical stresses (N/mm²) for proposed section**

Figure 8 shows time history of major principal stress at the heel of the dam for one of the selected near-fault earthquake record, which rises up repeatedly above static demand capacity ratio (DCR) and dynamic DCR.



**Figure 8: Time history of major principal stress at the heel of the dam for Imperial Valley-06 (Recording station: El Centro Array#6) Earthquake (FN + V)**

Result shows that factor of safety in sliding fall repeatedly below one for near-field records which confirmed that, at that time dam will undergo sliding at the base (Figure 9).
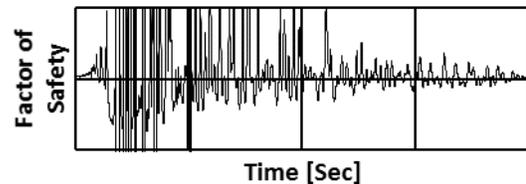


**Figure 9: Time history of instantaneous factor of safety for near-field earthquake (NGA#1084)**

Figure 10 shows response of fifteen selected near-field earthquakes and five far-field earthquakes. Response due to far-field earthquakes are within the performance limit while the response due to all the near-field earthquakes are quite outside from the performance limit. One important point to be noted from the above Figure 10 that, the earthquake time history which has large peak velocity is more damaging than that having less velocity though that has large peak acceleration. As in above chart NGA#1106 with PGA = 0.85g and PGV = 96.27 cm/s is more damaging than NGA#825 with PGA = 1.27g and PGV = 59.55 cm/s. This suggests that care should be taken during the selection of earthquakes data while working with near-field earthquake time histories.
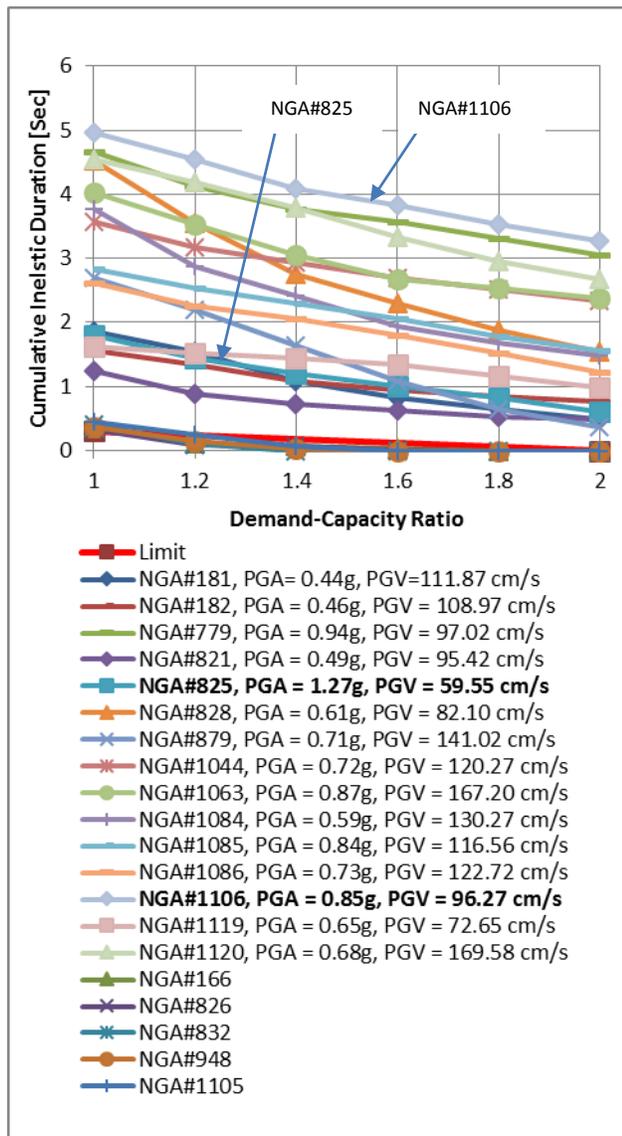


**Figure 10: Comparison of cumulative duration of stress cycle with acceptance stresses at the heel of the dam**

## 6. Non-Linear Time History Analysis

The results of linear analysis show that high tensile stresses develop at the base of the dam, on the upstream face, and on the downstream face near the change of slope [7]. The magnitudes of stresses are generally higher at the base of the dam than at the upper elevations. For this reason and also because tensile strength of the dam-rock contact is expected to be lower than that of the concrete, the nonlinear response in the form of tensile cracking is likely to start at the base of the dam. The nonlinear analysis of the dam should therefore be formulated to capture this nonlinear behavior. In this study, gap-friction elements are introduced at the base of the dam to simulate cracking and sliding response of the dam.

The dynamic equilibrium equations of a linear elastic structure with predefined nonlinear Link/Support elements [8] subjected to an arbitrary load can be written as:

$$K_L u(t) + C \dot{u}(t) + M \ddot{u}(t) + r_N(t) = r(t) \qquad .......... (4)$$

Where $K_L$ is the stiffness matrix for the linear elastic elements (all elements except the Links/Supports); C is the proportional damping matrix; M is the diagonal mass matrix; $r_N$ is the vector of forces from the nonlinear degrees of freedom in the Link/Support elements; u, $\dot{u}$, and $\ddot{u}$ are the relative displacements, velocities, and accelerations with respect to the ground; and r is the vector of applied loads.

Finite-element model for the nonlinear analysis consists of the dam monolith and gap-friction elements. The foundation rock is not included in the model in order to reduce computational efforts. The tensile cracking at the base of the dam is modelled by introducing gap-friction elements between the dam and the rigid foundation. The gap-friction elements are nonlinear elements that can resist bearing and shear parallel to the bearing plane but not tension. The friction forces follow the Coulomb theory and thus are directly proportional to bearing forces in the element. Figure 11 shows the dam finite-element model with 51 gap-friction elements between the dam and the rigid base. Except for the nonlinear gap-friction elements, the rest of the dam is assumed to remain elastic. Consequently, the dam monolith is represented by linear finite elements. The complete finite element model consists of 8050 linear plane elements with 51 nonlinear gap-friction elements [7].

The behavior of the gap-friction element is both complex and nonlinear. Figure 12 shows the idealized constitutive relations of the gap-friction element in the

normal and tangential direction. The gap-friction element behavior can be characterized as elastic-perfectly plastic, and incapable of withstanding any tensile stress in normal direction [9].
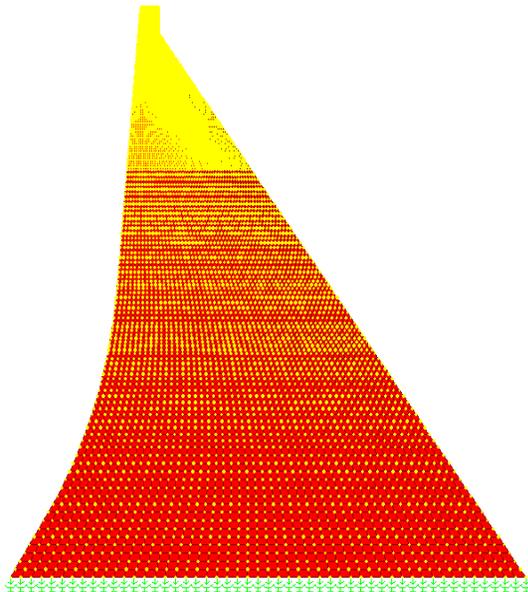


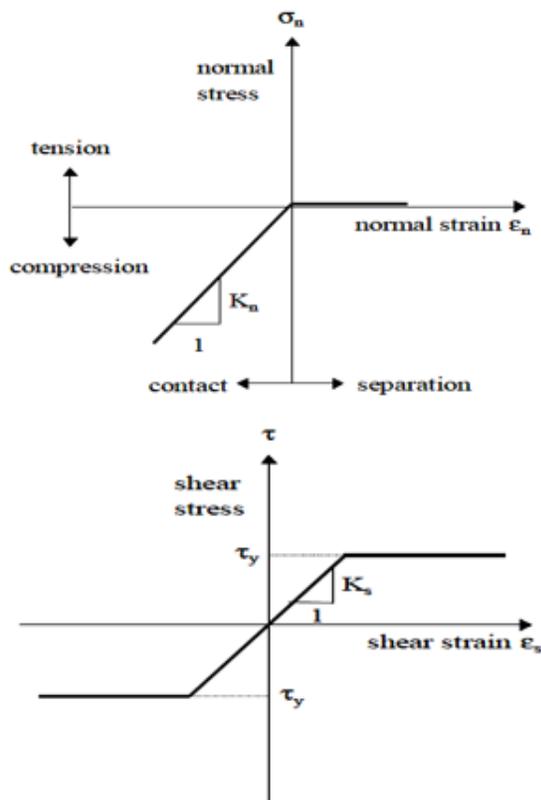**Figure 11: Dam finite element model with gap-friction elements**

The tangential stress-strain relationship is assumed to be elastic-plastic, based on the Mohr-Coulomb yield criterion:

$$\tau_y = c + \sigma_n \tan \phi \qquad \cdots\cdots (5)$$

Where, c and $\phi$ denote cohesion and the friction angle respectively.

Figure 13 shows deflected shape at the time of maximum displacement. Thirty one gap-friction elements in the upstream side opened and slide during the earthquake ground shaking at the time of maximum displacement. This indicates that cracking starts at the heel of the dam and stops after propagating about half with of the base. Figure 14 shows time histories of sliding displacements for joints at heel and toe across the base of the dam. The sliding displacements are slightly higher for nodes closer to the heel and reduce as approaching the toe. The result shows an overall permanent sliding displacement of about 40 mm. Figure 15 shows the horizontal displacement history at the top of the dam, where the permanent displacement at the end of the record is about 25 mm.
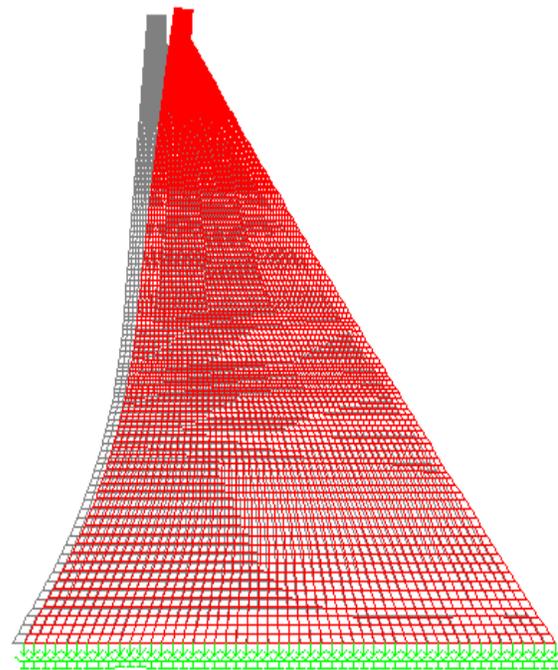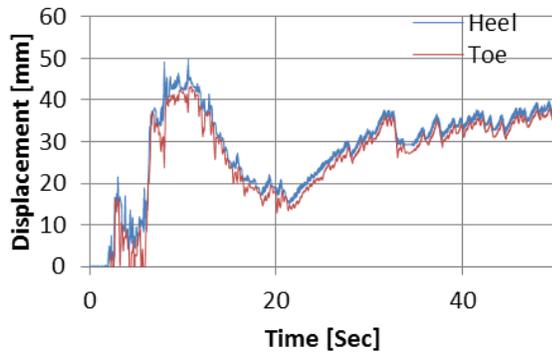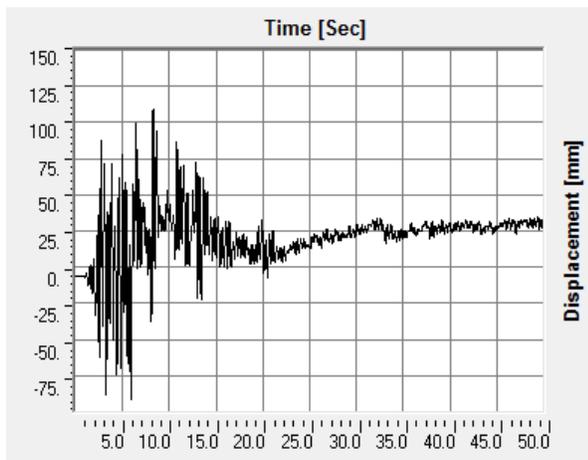


**Figure 13: Dam finite-element model with gap-friction elements**



**Figure 12: Constitutive relations of gap-friction element**

*Nonlinear time history analysis of large concrete dam considering near-field earthquake effect*

**Figure 14: Time history of sliding displacements of nodal points (heel and toe) at the base of dam (NGA#1120)**



**Figure 15: Time history of horizontal displacement at the top of dam (NGA#1120)**

## 7.  Conclusion

This study concludes that near-field earthquakes are several times destructive than the far field earthquakes. This study also concludes that peak ground velocity (PGV) and frequency contents of ground motion records are also equally responsible along with peak ground acceleration (PGA) for the damage of the large structures specially located in near fault.

This concludes that while performing the analysis of large dam structures in tectonically active country like Nepal, it would be more appropriate to use the near-field records than code based earthquake evaluation method or far field earthquake records.

## References

[1]  C. A. Maniatakis, I. Taflampas and C. Spyrakos, "Identification of Near-Fault Earthquake Record Characteristics," in *The 14th World Conference on Earthquake Engineering*, Beijing, China, 2008.

[2]  "PEER," 2013. [Online]. Available: peer.berkeley.edu/peer_ground_motion_database. [Accessed 2013].

[3]  A. Palmstrom and R. Singh, "THE DEFORMATION MODULUS OF ROCK MASSES-comparisions between in situ tests and indirect estimates," *Tunnelling and Underground Space Technology, Vol. 16, No. 3,* p. 20, 2001.

[4]  U. A. C. o. E. "Time-History Dynamic Analysis of Concrete Hydraulic Structures, EM 1110-2-6051," 2003.

[5]  U. A. C. o. E. "Earthquake Design and Evaluation of Concrete Hydraulic Structures, EM 1110-2-6053," 2007.

[6]  R. W. Clough and J. Penzien, Dynamics of Structures, Third Edition, Berkeley: Computers and Structures, Inc., 1995.

[7]  US Army Crops of Engineers, "Earthquake Design and Evaluation of Concrete Hydraulic Structures, Engineering Manual, EM 1110-2-6053," US Army Crops of Engineers, Washington, DC, 1 May 2007.

[8]  Computers and Structures, Inc., CSI Analysis Reference Manual for SAP2000, ETABS, SAFE and CSiBridge, Berkeley, California, USA: Computers and Structures, Inc., March 2013.

[9]  A. Tzamtzis and P. Asteris, "FE Analysis of Complex Discontinuous and Jointed Structural Syatems," *Electronic Journal of Structural Engineering, 1,* p. 18, 2004.